

# Spectral sensitivity differences between rhesus monkeys and humans: implications for neurophysiology

Zachary Lindbloom-Brown, Leah J. Tait, and Gregory D. Horwitz

Department of Physiology and Biophysics and Washington National Primate Research Center, University of Washington, Seattle, Washington

Submitted 12 May 2014; accepted in final form 17 September 2014

**Lindbloom-Brown Z, Tait LJ, Horwitz GD.** Spectral sensitivity differences between rhesus monkeys and humans: implications for neurophysiology. *J Neurophysiol* 112: 3164–3172, 2014. First published September 24, 2014; doi:10.1152/jn.00356.2014.—Spectral sensitivity of humans and rhesus monkeys was compared using identical displays and similar procedures. Detection thresholds were measured for the following: 1) 15-Hz modulation of a blue and a green cathode-ray tube phosphor; 2) 15-Hz modulation of all three phosphors together; and 3) slow (<1 Hz) modulations of a blue and a green phosphor under scotopic conditions. Monkeys had lower blue-to-green threshold ratios than humans at all eccentricities tested (0.5 to 7°), consistent with a lower lens optical density in monkeys. In addition to apparently having a lower lens density than humans, monkeys were more sensitive to 15-Hz red-green isoluminant modulations than humans, an effect that cannot be explained by optical factors.

monkey; color; luminance; cone fundamentals

THE TOOLS OF VISION SCIENCE include psychophysical experiments in humans and neurophysiological experiments in monkeys. Establishing direct links between these two types of investigation requires that psychophysical performance of monkeys is similar to that of humans, and that neural responses measured in humans are similar to those measured in monkeys. We tested the first proposition by comparing human and monkey contrast detection thresholds under photopic and scotopic conditions.

Our study extends the pioneering work of De Valois, Jacobs and others, who compared the spectral sensitivities of human observers against several species of monkey (De Valois et al. 1974; De Valois and Jacobs 1968; De Valois and Morgan 1974; Harwerth and Smith 1985; Jacobs and Deegan 1997; Schrier and Blough 1966; van Norren 1971). Although the result was not emphasized, these studies found that macaques are more sensitive to short-wavelength lights than humans (Fig. 1). We probed the significance of this result for visual neurophysiology by focusing exclusively on *Macaca mulatta* (rhesus monkeys), which has become a standard model for neurophysiological studies in the field. We also enforced visual fixation in our psychophysical tasks to distinguish the role of macular pigment in shaping spectral sensitivity from other factors.

We considered prereceptoral, receptoral, and postreceptoral explanations for the monkeys' relatively high sensitivity to short-wavelength light. The prereceptoral factors included dif-

ferences in the optical density of the lens and macular pigment. We tested and rejected the receptor-based explanation that a greater proportion of M-cones in the monkey eye mediated their greater short-wavelength sensitivity. We also considered the possibility that, in monkeys, cone-opponent mechanisms contributed to the detection of rapidly flickering patterns that, in humans, are detected by a weighted sum of L- and M-cone signals.

We conducted three experiments. *Experiment 1* confirmed that monkeys are more sensitive to short-wavelength lights than humans are, and it showed that this sensitivity difference extends into the visual periphery, undermining explanations based on macular pigment density. *Experiment 2* showed that detection of the patterns used in *experiment 1* was mediated dominantly by a linear, univariate luminance mechanism, supporting the idea that sensitivity differences in *experiment 1* were due to preretinal factors. *Experiment 3* showed that differences in scotopic detection thresholds were consistent with a lower lens density in monkeys.

## METHODS

**Subjects.** Five *Macaca mulatta* monkeys and three human subjects participated in these experiments. Sex and ages (yr) for each subject are as follows: *human G* (man/42), *human Z* (man/25), *human L* (woman/24), *monkey A* (male/7), *monkey F* (female/6), *monkey K* (female/9), *monkey N* (female/3), and *monkey S* (female/9). All monkeys were of Indian origin, and all procedures used with them were approved by the University of Washington Institutional Animal Care and Use Committee and adhered to the American Physiological Society's Guiding Principles for the Care and Use of Vertebrate Animals in Research and Training. All human subjects were Caucasian, and all procedures used with them conformed to the Declaration of Helsinki and the policies of the University of Washington Human Subjects Division. Human subjects provided written, informed consent.

**General.** Humans and monkeys viewed the same display in the same testing booth. Monkeys were head-fixed and reported psychophysical judgments by making saccades to targets that appeared at the end of each trial. Humans were not head-fixed and reported judgments with button presses. For humans, correct responses were indicated with a tone, and eye position was not measured. For monkeys, correct responses were reinforced with a tone and a drop of apple juice, and eye position was measured with a monocular scleral search coil. Stimuli in all experiments were generated in MATLAB (MathWorks) with functions from The Psychophysics Toolbox (Brainard 1997; Kleiner et al. 2007; Pelli 1997).

For most experiments, stimuli were presented on a cathode-ray tube (CRT) monitor (Sony Trinitron) updated at 75 Hz and rendered at a color depth of 14 bits per color channel using a digital video processor (Bits++, Cambridge Research Systems). To extend the range of stimulus contrasts available, a subset of data for *experiment 2* were

Address for reprint requests and other correspondence: G. D. Horwitz, Dept. of Physiology and Biophysics & Washington National Primate Research Center, Univ. of Washington, 1959 NE Pacific St., HSB 1-728, UW Mailbox: 357290, Seattle, WA 98195 (e-mail: ghorwitz@u.washington.edu).

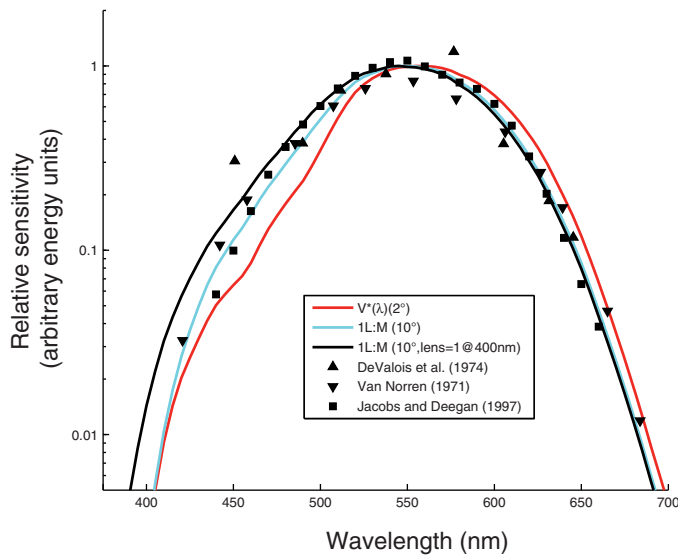


Fig. 1. Spectral sensitivity data from rhesus monkeys (symbols) and spectral sensitivity functions for three theoretical observers (curves). Curves represent a 1.98L+M weighted sum of the  $2^\circ$  Stockman and Sharpe cone fundamentals,  $V^*(\lambda)$  (red), 1L+1M of the  $10^\circ$  cone fundamentals (cyan), and 1L+1M of the  $10^\circ$  cone fundamentals with a reduced lens density [optical density (OD) = 1 at 400 nm; black]. Each set of symbols has been shifted vertically to minimize the sum of their squared distance to the cyan curve at wavelengths  $\geq 540$  nm. Data were captured digitally (van Norren 1971; De Valois et al. 1974; Jacobs and Deegan 1997). The van Norren data are electroretinogram flicker photometric thresholds (40 Hz, Maxwellian view,  $45^\circ$  subtense). The De Valois et al. data are behavioral detection thresholds (25 Hz, Newtonian view, at a variable distance from the subject). The Jacobs and Deegan data are electroretinogram flicker photometric nulls (31.25 Hz, Maxwellian view,  $57^\circ$  subtense).

collected using a wide-gamut liquid-crystal display (LCD) that updated at 120 Hz and had a color depth of 10 bits per color channel (VPixx Technologies). The gamut of the LCD display was larger than the CRT's in the L-M direction, allowing us to achieve simultaneous L- and M-cone contrasts in the range of  $\pm 0.171$  instead of  $\pm 0.094$ , but was smaller in the S-cone isolating direction, with a maximal S-cone contrast of 0.81 instead of 0.88. The background was an equal energy white metamer ( $x = 0.3, y = 0.3$ ) at  $\sim 100$  cd/m $^2$  on the CRT and  $\sim 50$  cd/m $^2$  on the wide-gamut display. Both monitors were viewed at a distance of 100 cm. Light emission spectra for both displays were measured with a PR705 spectroradiometer (PhotoResearch; Fig. 2). Data described in this report are available for download from <http://www.github.com/horwitzlab>.

**Detection task.** Humans and monkeys performed a spatial two-alternative forced choice contrast detection task that our laboratory has used previously (Hass and Horwitz 2011, 2013). On each trial, the subject fixated a  $0.2^\circ$  black point in the center of the monitor. Five hundred milliseconds later, a Gabor stimulus appeared on the horizontal meridian either to the right or to the left of the fixation point. The subject's task was to indicate on which side of the fixation point the stimulus appeared. Stimulus eccentricities varied from  $0.5$  to  $7^\circ$  across blocks of trials. Contrasts were adjusted by the QUEST algorithm to find the subject's detection threshold (Watson and Pelli 1983). At the end of each trial, a pair of targets appeared  $5^\circ$  from the fixation point. For monkeys, a saccade to the target in the direction of the Gabor stimulus was counted as a correct response. Humans were instructed to press the button on the same side of a handheld button box as the Gabor stimulus. Each threshold measurement was based on 40 trials for humans and 80 trials for monkeys, and 1 to 13 thresholds were averaged at each eccentricity.

The sinusoidal component of the Gabor stimulus was oriented horizontally, had a spatial frequency of 3 cycles/ $^\circ$ , and drifted up-

wards at 15 Hz. The Gaussian envelope had a standard deviation of  $0.15^\circ$ . The contrast ramped up linearly over 160 ms, remained constant for 347 ms, and then ramped down again over 160 ms (12, 26, and 12 CRT monitor refreshes, respectively). By convention, the contrast of the stimulus was defined as (peak - mean)/mean during the 347-ms plateau.

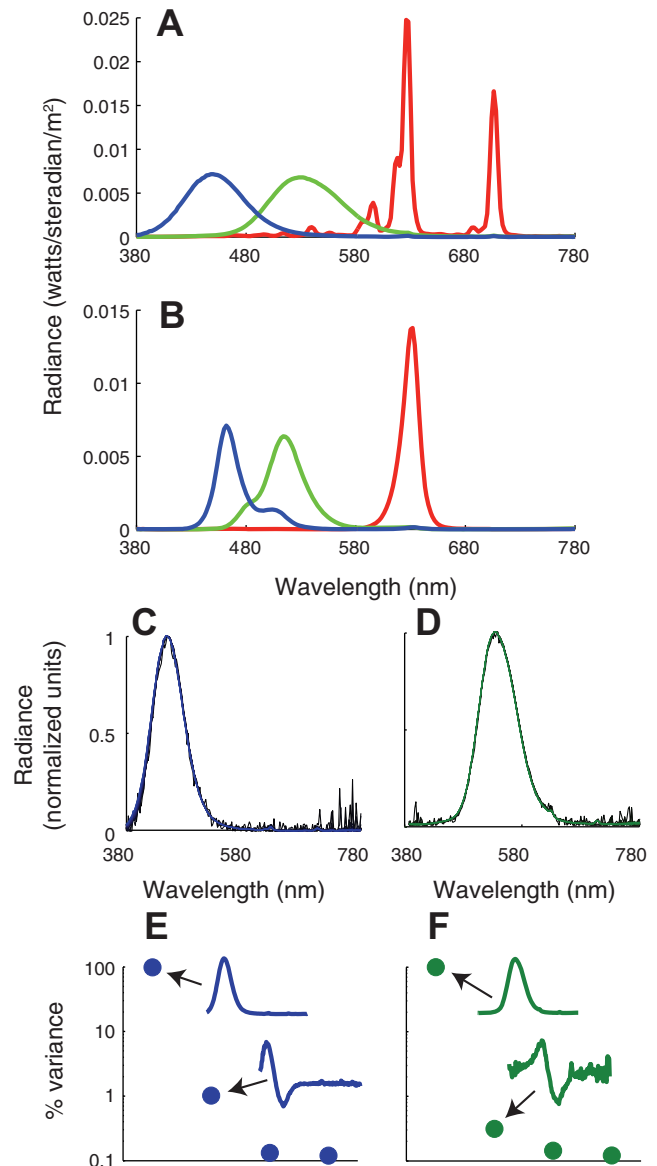


Fig. 2. Light emission spectra from the cathode-ray tube (CRT; A) and wide-gamut liquid-crystal display (LCD; B) measured on the gray background used in *experiments 1* and *2*. Commission Internationale de l'Éclairage chromaticity coordinates ( $x, y$ ) for each light are as follows: red<sub>CRT</sub> (0.63, 0.34), green<sub>CRT</sub> (0.29, 0.61), blue<sub>CRT</sub> (0.15, 0.07), red<sub>LCD</sub> (0.69, 0.30), green<sub>LCD</sub> (0.14, 0.63), blue<sub>LCD</sub> (0.14, 0.10). Modulation of the blue CRT phosphor on the equal energy white background produced cone contrasts in ratios 0.11:0.20:0.97 (L/M/S). Modulation of the green CRT phosphor produced cone contrasts in ratios 0.63:0.77:0.08. C: blue CRT phosphor spectra measured at 30 intensity values spanning the dynamic range. Each overlaid spectrum was corrected for ambient light (the dark light spectrum was subtracted) and normalized to peak at 1. D: same as C, but for the green phosphor. E: percentage of total variance accounted for by the four largest eigenvectors from a singular value decomposition of the matrix of spectral measurements. The largest two eigenvectors are shown in *insets*. F: same as E, but for the green phosphor.

**Luminance threshold ratio predictions.** In *experiment 1*, the Gabor stimulus was produced by modulation of the green and blue CRT phosphors in interleaved trials. We measured blue and green contrast thresholds and computed the ratio of these quantities to quantify short-wavelength (blue) sensitivity relative to a longer wavelength (green) benchmark. Threshold ratios from our human and monkey subjects were compared with predictions from several theoretical observers, which were obtained via the equations:

$$B = \frac{\sum_{\lambda} V^*(\lambda) \cdot I_{blue}(\lambda)}{\sum_{\lambda} S(\lambda) \cdot I_{blue}(\lambda)} \quad (1)$$

$$G = \frac{\sum_{\lambda} V^*(\lambda) \cdot I_{green}(\lambda)}{\sum_{\lambda} S(\lambda) \cdot I_{green}(\lambda)} \quad (2)$$

where  $I_{green}(\lambda)$  and  $I_{blue}(\lambda)$  are the emission spectra of the green and blue phosphors measured at full intensity, respectively;  $S(\lambda)$  is the spectral sensitivity of a theoretical observer; and  $V^*(\lambda)$  is a human luminous efficiency function under daylight adaptation (Sharpe et al. 2005, 2011). The ratio, B/G, is the blue-to-green threshold ratio for the theoretical observer. This quantity equals 1 for an observer whose sensitivity to blue and green modulations is well described by the human luminous efficiency function, it is  $> 1$  for an observer that is more sensitive to modulations of the green phosphor, and it is  $< 1$  for an observer that is more sensitive to modulations of the blue phosphor.

We estimated lens optical density for individual subjects from B/G, pooling data from eccentricities  $\geq 5^\circ$  where macular pigment is nearly absent (Snodderly et al. 1984a, 1984b; Wooten and Hammond 2005). The theoretical observer's spectral sensitivity was given by a weighted sum of L- and M-cone Stockman and Sharpe  $10^\circ$  fundamentals. The weights on the L- and M-cone fundamentals were set to 1:1 for all monkeys and for *human G* and to 10:1 for *humans Z* and *L*. These ratios were selected on the basis of data from *experiment 2* (see Fig. 4), electroretinogram data from the human subjects (data not shown), and measurements of L-to-M ratio across a large population of rhesus monkeys (Jacobs and Deegan 1997, 1999). Lens optical density of the theoretical observer was adjusted until the B/G of the theoretical observer matched the B/G of the subject.

**Isodetectability measurements.** In *experiment 2*, we used the two-alternative forced choice contrast detection task to measure isodetectability surfaces. Isodetectability surfaces are collections of stimuli, in cone contrast space, that are equally detectable to a psychophysical observer. In this experiment, the Gabor stimulus appeared  $5^\circ$  from the fixation point along the horizontal meridian. All three phosphors modulated simultaneously in ratios that defined the color direction of the stimulus. Color directions were selected using an adaptive algorithm, the full details of which can be found in a previous publication (Horwitz and Hass 2012). In this earlier study, we used the algorithm to measure isoresponse surfaces of V1 neurons; here we use it to measure isodetectability surfaces of psychophysical observers.

To measure points on an isodetectability surface, we measured detection thresholds in three interleaved color directions using the QUEST procedure. Initial color directions were the L-M, L+M+S, and S directions of cone contrast space. Subsequent color directions were chosen to sample regions of the space in which the isodetectability surface was curved. Detection thresholds were fit with a modified version of the model of Cole et al. (1993):

$$\sum_{i=1}^2 \left( \left| l_i \frac{\Delta L}{L} \right| + \left| m_i \frac{\Delta M}{M} \right| + \left| s_i \frac{\Delta S}{S} \right| \right)^\beta = 1 \quad (3)$$

Under this model, detection is mediated by a pair of linear mechanisms whose output is combined by nonlinear pooling. A single linear mechanism described the monkey data inadequately, and a three-mechanism model was unnecessarily complex. In Eq. 3,  $l_i$ ,  $m_i$ , and  $s_i$  are the weights on the L-, M-, and S-cone contrasts ( $\Delta L/L$ ,  $\Delta M/M$ ,

and  $\Delta S/S$ ) associated with the  $i$ th detection mechanism, respectively, and  $\beta$  is a pooling parameter that indicates the degree of interaction among the mechanisms. The seven parameters were fit by minimizing the absolute log radial error between the threshold measurements and the surface. For the purposes of fitting, thresholds that exceeded the monitor gamut did not contribute to the error unless the model predicted a lower threshold, in which case the threshold was defined as the highest contrast tested in that color direction.

**Scotopic detection.** To measure scotopic thresholds, we covered the center  $285 \times 90$  mm of the CRT monitor screen with 6 log-units of neutral density filter (Kodak Wratten 96) and the remainder of the screen with light absorbent materials. Subjects dark adapted for 20–40 min before the first threshold measurement. Six to thirteen threshold measurements were made in each session.

The background of the screen was set to a nominal black (8 photopic  $\text{cd/m}^2$  before the filters,  $5 \times 10^{-6}$  scotopic  $\text{cd/m}^2$  after), and stimuli were  $2 \times 2^\circ$  squares with centers located  $7^\circ$  to the left or right of the fixation point, presented for 667 ms. A  $6^\circ$  diameter white ring at the center of the display served as a fixation target (a  $< 1^\circ$  portion of the ring was obscured by the occluder).

We measured the emission spectrum of each monitor phosphor on the black background with a PR705 spectroradiometer (PhotoResearch) and multiplied each by the transmission spectrum of the neutral density filters. Transmission spectral data were available from the manufacturer for a 1.0 log unit filter only (Kodak 1990). To account for the fact that we used 6.0 log units of neutral density filter (2 filters, each of which provided 3.0 log units of attenuation), we raised the transmission spectrum of the 1.0 log unit filter to an exponent of 6. We confirmed the accuracy of the manufacturer's specifications of the 1.0 log unit filter by direct measurement.

To estimate lens optical density from scotopic B/G for each observer, we divided the Commission Internationale de l'Éclairage scotopic luminous efficiency function,  $V'(\lambda)$ , by the Stockman and Sharpe lens transmittance spectrum (Stockman et al. 1999) to estimate a rod absorbance spectrum. We then scaled the Stockman and Sharpe lens density spectrum, converted it to transmittance, and multiplied it by the rod absorbance spectrum to derive a corneal rod fundamental. B/G for a scotopic theoretical observer was calculated as the ratio of dot products between this fundamental and the emission spectra of the blue and green phosphors. Scotopic trolands were calculated assuming an 8-mm diameter pupil (Wyszecki and Stiles 1982).

## RESULTS

**Photopic sensitivity to short- and medium-wavelength flicker.** Monkey photopic detection thresholds were similar to those of humans, showing that the monkeys were well-trained, motivated psychophysical observers (Fig. 3). As expected from the drop in cone density outside of the fovea, thresholds for all subjects increased with retinal eccentricity.

B/G of human subjects were broadly consistent with photometric luminance sensitivity. Near the fovea, B/G of all human observers was slightly higher than 1. This is expected because threshold is quantified in units of  $2^\circ$  nominal human luminance contrast, based on a luminous efficiency function that is appropriate for a  $2^\circ$  field centered on the human fovea (Sharpe et al. 2011; Stockman and Sharpe 2000). B/G of human observers decreased with eccentricity and was close to  $\sim 0.9$  at  $7^\circ$  of eccentricity. This decrease is due to that fact that  $V^*(\lambda)$  underestimates short-wavelength sensitivity outside of the central  $2^\circ$ , where macular pigment is sparse.

Monkeys were more sensitive to blue, relative to green, than the human subjects. Differences in B/G between humans and monkeys were pronounced even  $7^\circ$  from the fovea (unpaired  $t$ -test,  $P < 0.01$ ). These data confirm that monkeys are more

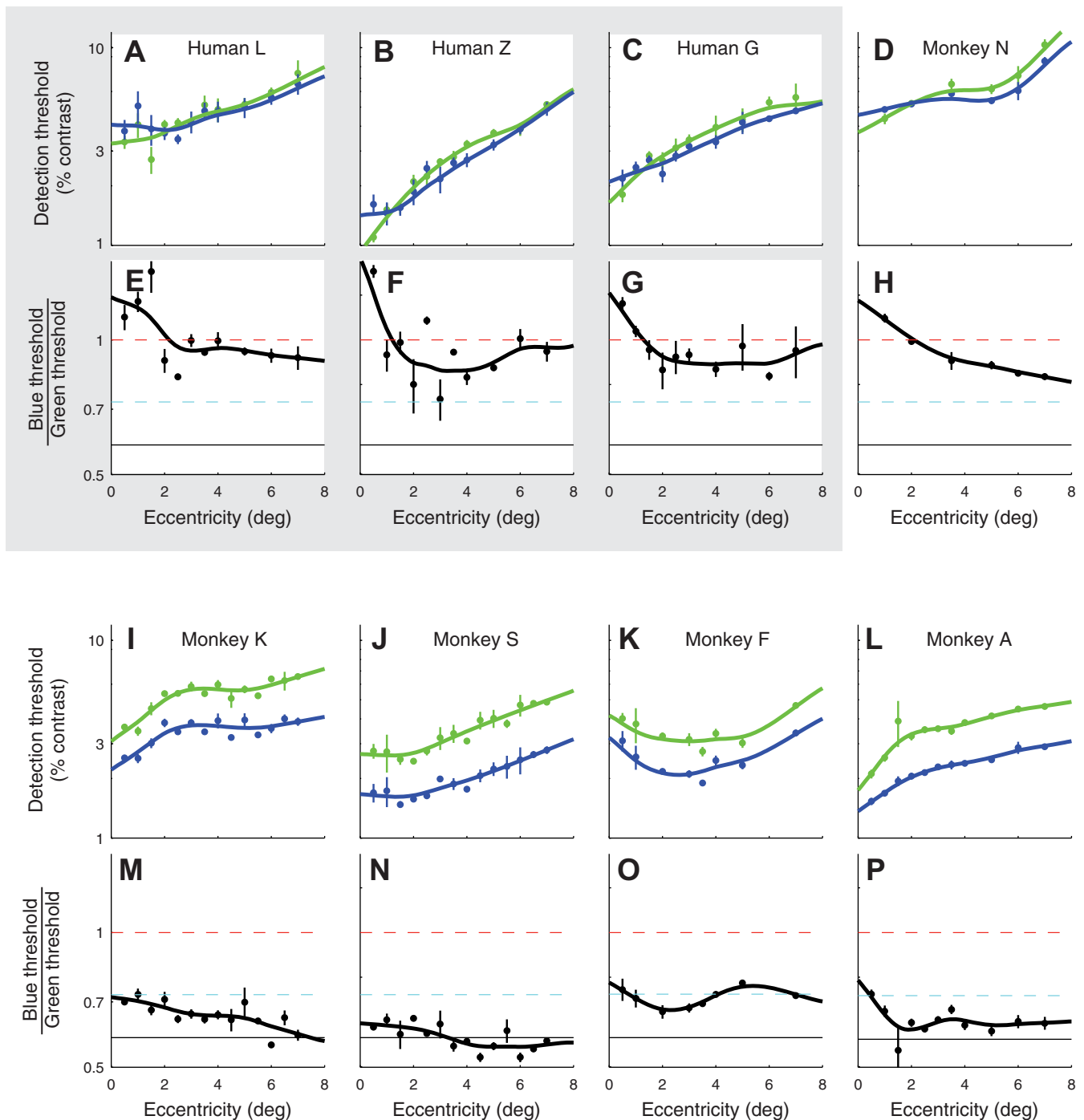


Fig. 3. Detection thresholds for 15-Hz modulations of the blue and green phosphor for 3 human subjects (shaded region; A–C, E–G) and 5 monkey subjects (nonshaded region; D and H–P). For each subject, *top* panels (A–D and I–L) show thresholds (blue and green points) and smoothing spline fits (curves). *Bottom* panels (E–H and M–P) show the ratio of blue and green thresholds (black dots) and the ratio of the fitted splines (curves). Dashed lines in *bottom* panels illustrate the spectral sensitivity of the three theoretical observers from Fig. 1 (red:  $2^\circ$  1.98L+M fundamentals, cyan:  $10^\circ$  L+M fundamentals, black:  $10^\circ$  L+M fundamentals with lens density = 1 at 400 nm). Error bars are SE.

sensitive to short-wavelength light than humans are (when short-wavelength sensitivity is expressed relative to longer wavelength sensitivity), and this difference cannot be attributed to differences in macular pigment density.

In humans, 15-Hz flicker is detected by a single, univariate linear mechanism that receives input from the L- and M-cones and little if any input from S-cones under conditions like ours (Eisner and MacLeod 1980; but see Stockman et al. 1991). The

proportion of L- to M-cone input to this luminance mechanism varies across observers, and much of this variation can be attributed to individual differences in the proportion of L- and M-cones in the eye (Brainard et al. 2000; Chang et al. 1993; Kremers et al. 2000) or to preretinal filters (Hammond et al. 2005; Wooten et al. 2007). To model expected changes in B/G with L-to-M-cone (L/M-cone) ratio and preretinal filter density, we calculated B/G for three theoretical observers with



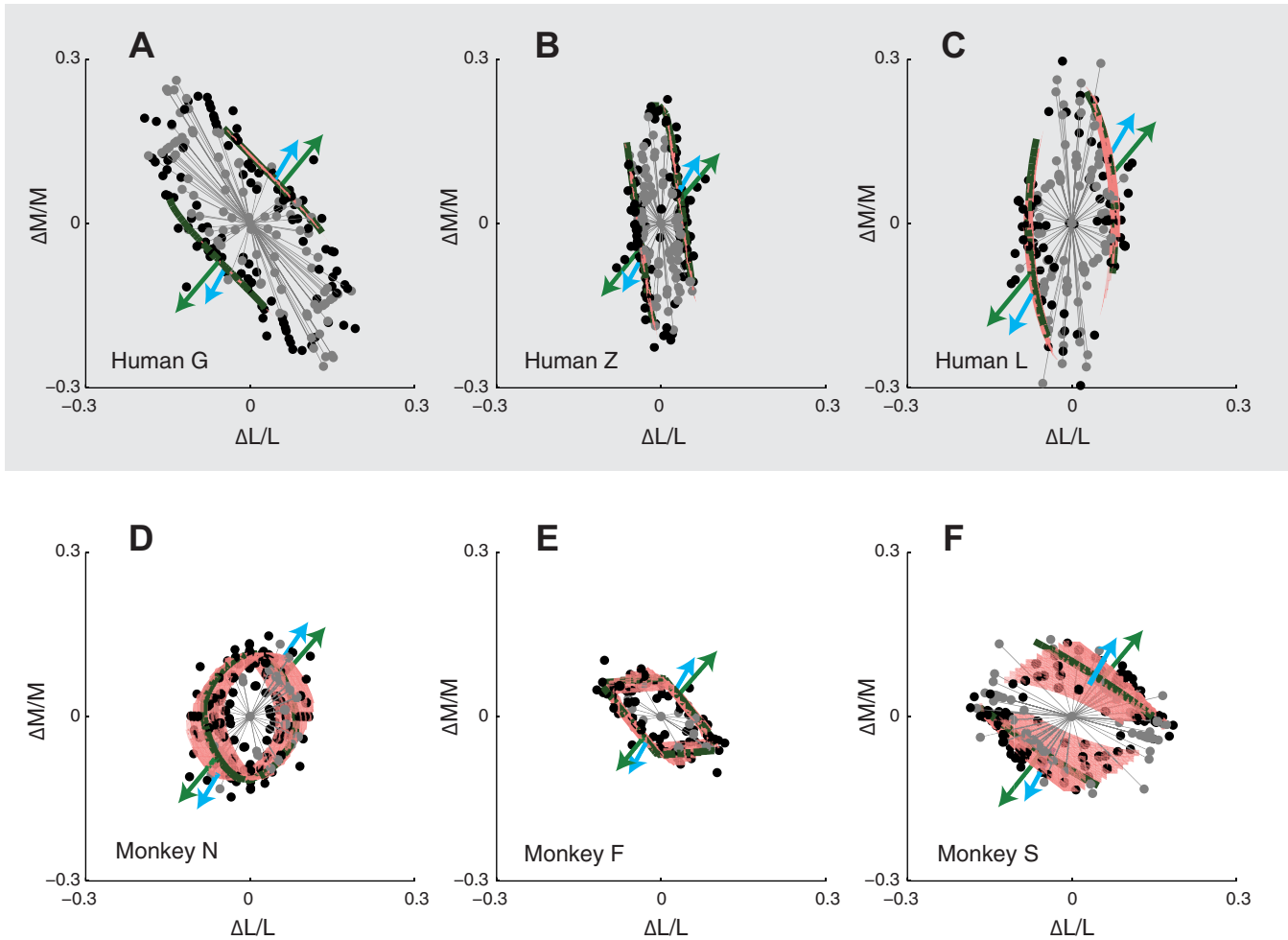


Fig. 4. Isodetectability surfaces in cone contrast space for three human (A–C) and three monkey (D–F) observers. Individual threshold measurements are represented as black dots, and fitted surfaces are shaded red. Gray lines and points indicate color directions in which thresholds were unmeasurable. Green and blue arrows show the color directions of the green and blue phosphor modulations, respectively. Dark green contours show the intersection of the isodetectability surface and the LM plane.

spectral sensitivity given by weighted sums of L- and M-cone fundamentals (Stockman and Sharpe 2000). One had a 1.98:1 L/M-cone ratio and a high macular pigment density, one had a 1:1 L/M-cone ratio and a low macular pigment density, and one had a 1:1 L/M-cone ratio and low macular pigment and lens densities (red, cyan, and black curves in Fig. 1 and dashed lines in Fig. 3). The monkeys' heightened sensitivity to blue cannot be explained solely based on a 1:1 L/M-cone ratio: B/G for monkeys was usually lower than the B/G predicted for a theoretical observer with a 1:1 L/M-cone ratio. Of the three theoretical observers we considered, the one with a 1:1 L/M-cone ratio and a reduced lens density was the most consistent with the monkeys' performance (Figs. 1 and 3).

The results of *experiment 1* are consistent with the idea that monkeys have lower lens optical density than humans. This interpretation, however, depends on the assumption that, for each observer, the 15-Hz green and blue phosphor modulations were detected by a single univariate linear mechanism. *Experiment 2* tests and supports this assumption.

**Isodetectability surfaces: 15 Hz.** To ask whether blue and green phosphor modulations were detected by a single mechanism or multiple mechanisms, we measured detection thresholds in a broad range of color directions. The geometric

arrangement of these thresholds, represented as points in three-dimensional cone contrast space, carries information about the number and tuning of the mechanisms that mediate detection (Cole et al. 1993; Eskew et al. 1999; Gegenfurtner and Hawken 1995). Note, however, that when more than one mechanism contributes to detection, estimating their number and tuning can be complicated, or even impossible, depending on how they interact (Poirson et al. 1990).

Table 1. Best fit parameter values for the model in Eq. 3

	Monkey N	Monkey F	Monkey S	Human G	Human Z	Human L
$\beta$	1.6452	0.9998	1.8091	5.9992	7.9172	1.8672
$\beta$ (SE)	0.4341	0.3053	0.1926	3.3464	16.3978	1.1583
$l_1$	0.0197	0.0751	0.0349	0.0817	0.2417	0.1266
$m_1$	0.0851	0.1362	0.0869	0.0801	0.0341	0.0016
$s_1$	-0.0010	0.0009	0.0096	-0.0002	0.0008	-0.0015
$l_2$	0.1168	0.0854	0.0560	0.0614	0.0024	-0.0014
$m_2$	-0.0141	-0.0073	0.0461	-0.0044	-0.0463	-0.0377
$s_2$	-0.0057	-0.0034	-0.0014	0.0007	0.0014	-0.0001

The standard error of the parameter,  $\beta$ , was estimated by bootstrapping raw threshold measurements (200 resamples). See text for definition of terms.

Detection thresholds for each observer were fit with a model that specifies isodetectability surfaces in cone contrast space (Eq. 3). Isodetectability surfaces for human subjects were roughly planar, consistent with modulations in all color directions being detected by a single, linear mechanism. For monkeys, however, isodetectability surfaces were curved, indicating that at least two mechanisms contributed to detection. For two of the three monkeys, the intersection of the isodetectability surface and the LM plane formed a closed contour. These monkeys, unlike the humans, could detect 15-Hz flicker in all directions in the LM plane (Fig. 4). All subjects except *monkey N* had a dominant detection mechanism with large, positive L- and M-cone weights and small S-cone weights (Table 1). L- and M-cone weights for the human subjects ( $\sim 1:1$  for *human G* and  $10:1$  for *humans Z* and *L*) were confirmed by electroretinographic measurement (data not shown).

Isodetectability surfaces contain the threshold cone contrast modulations produced by the blue and green phosphors (Fig. 5 and Supplemental Movie S1; The online version of this article contains supplemental data). To characterize the tuning of the mechanisms that mediate detection of the phosphors, we inspected the shape of the isodetectability surface around and between their cone contrast directions (the blue phosphor modulates the S-cones most strongly, whereas the green phosphor modulates the L- and M-cones more strongly). For all

subjects, the isodetectability surface was relatively flat in this neighborhood and nearly parallel to the S-cone axis. The flatness of the surface indicates that modulations of the blue and green phosphor are detected by a common mechanism. The alignment of the surface to the S-cone axis indicates that the detection mechanism receives little if any input from the S-cones.

To confirm that blue and green phosphor modulations were detected by a common luminance mechanism, we performed two analyses. First, we compared model thresholds in the blue and green phosphor directions with and without the second mechanism ( $l_2$ ,  $m_2$ ,  $s_2$  in Table 1) included. Including the second detection mechanism changed the model's thresholds in the blue and green phosphor directions by an average of 15%, and B/G by an average of 17% (analysis applied to monkeys only; the same analysis applied to humans revealed much smaller changes). Second, we remeasured monkey isodetectability surfaces at 25 Hz, a frequency at which chromatic sensitivity was reduced (Fig. 5, *insets*). Planes fit to these 25-Hz detection data predicted B/G that differed from B/G measured in *experiment 1* by an average of 4%. These results show that the stimuli in *experiment 1* were dominantly detected by a single luminance mechanism, supporting the interpretation of the results of *experiment 1* in terms of preretinal filtering.

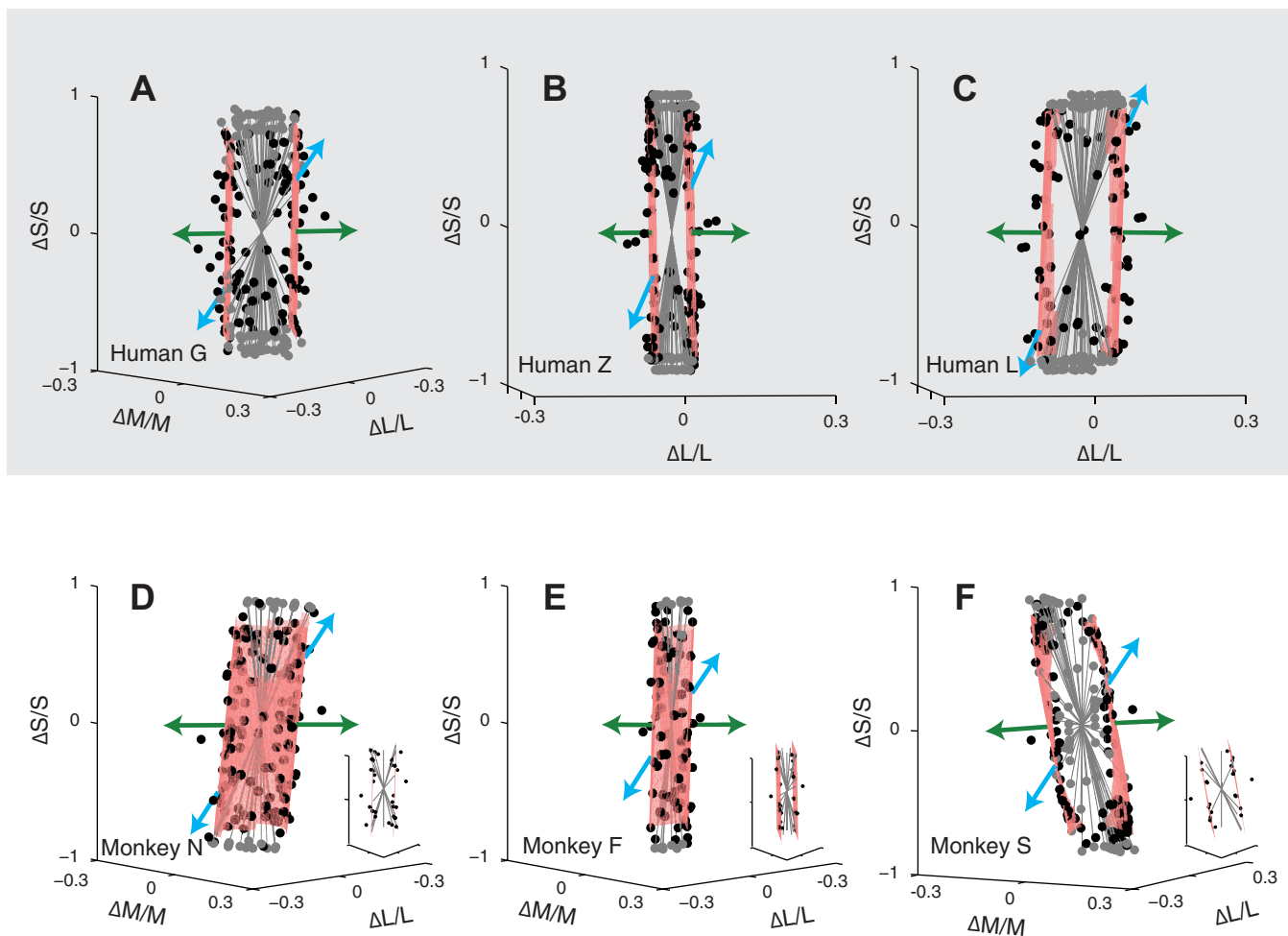


Fig. 5. Isodetectability surfaces. Data and fits are same as in Fig. 4, but have been projected onto the plane spanned by the green and blue phosphors. *Insets* in *D*, *E*, and *F* show isodetectability surfaces measured using 25-Hz stimuli.

**Scotopic detection.** As a further test of the hypothesis that monkey lenses are more transmissive than human lenses, we measured B/G at scotopic light levels. Scotopic detection is mediated by the rods only, and individual differences in scotopic spectral sensitivity are thought to be due primarily to individual differences in lens density (Crawford 1949; van Norren and Vos 1974).

Scotopic detection thresholds were noisy and did not differ significantly between monkeys and humans [monkeys:  $-3.65 \pm 0.12$  (mean  $\pm$  SD)  $\log_{10}$  scotopic trolands; humans:  $-3.70 \pm 0.09$   $\log_{10}$  scotopic trolands, unpaired *t*-test,  $P = 0.44$ ]. There was a trend, however: monkeys have lower scotopic B/G than humans, consistent with a lower lens density in this species (ANOVA with the random effect of subject nested within species:  $P = 0.084$ ). Lens optical density, estimated on the basis of scotopic and photopic B/G for individual subjects, was correlated ( $r = 0.87$ ,  $P = 0.02$ ) (Fig. 6).

## DISCUSSION

We compared the ability of human and monkey observers to detect 15-Hz flicker of a blue and green CRT phosphor as a function of retinal eccentricity. Consistent with previous studies, we found that monkeys were relatively more sensitive to blue flicker than humans. We could account for the monkeys' sensitivity to blue by assuming a 1:1 L/M-cone ratio and a lens optical density that is slightly below that of the average human. Below, we discuss our assumptions and consider alternative interpretations of the data. Then we discuss problems in cone weight estimation that can arise when human cone fundamentals are used to design visual stimuli for monkeys. Finally, we discuss the high sensitivity of monkeys to 15-Hz red-green

isoluminant flicker and its implications for neurophysiological experiments.

**Assumptions and alternative interpretations.** Our data support the idea that the monkeys' sensitivity to blue is due to preretinal filters that are more transmissive in this species than in humans. The two greatest sources of preretinal filtering are the macular pigment and lens. The fact that the monkeys' high sensitivity to blue flicker persists out to  $7^\circ$  of eccentricity suggests that the lens contributes significantly.

An alternative explanation for our data is that S-cones participate in the detection of 15-Hz flicker in monkeys but not in humans. While we cannot reject this idea outright, the weight of the evidence is against it. First, we observed a trend for lower scotopic B/G in monkeys, which cannot be mediated by the S-cones. Second, at high temporal frequencies, luminance modulations are thought to be detected by parasol cells, which do not receive S-cone input in monkeys (Field et al. 2010; Lee et al. 1989; Sun et al. 2006). Third, transient tritanopia reveals differences in human and monkey S-cone isolating color directions, a result that, like ours, can be explained by preretinal filtering (Hall and Colby 2013). An explanation based on species differences in both S-cone opponent (Hall and Colby 2013) and nonopponent (our study) pathways is less parsimonious.

Another possibility is that the spectral sensitivity of the cones themselves differs between monkeys and humans. One way in which this could occur is if monkey and human cones differ in axial photopigment density (higher densities broaden absorbance spectra). Such differences, if they exist, are bound to be small, and we confirmed that manipulating cone photopigment optical density from 0.2 to 0.4 was insufficient to account for the difference in B/G between humans and monkeys (data not shown).

Whereas L- and M-cones are very similar in monkeys and humans (Baylor et al. 1987; Bowmaker 1990), monkey S-opsin has a slightly longer maximum wavelength ( $\lambda_{\max}$ ) than human S-opsin (Bowmaker 1990; Dartnall et al. 1983; Harosi 1987; van Norren 1972). Removing the lens (1.765 at 400 nm) and macular pigment (0.095 at 460 nm) optical density spectra from the Stockman and Sharpe  $10^\circ$  S-cone fundamental reveals an absorbance spectrum that peaks at 420 nm (in quantal units), which is shorter than 430 nm, the approximate  $\lambda_{\max}$  of the macaque S-cone pigment (Bowmaker et al. 1978; Harosi 1987). Shifting the  $\lambda_{\max}$  of the S-cone absorbance spectrum by 10 nm prior to replacing the lens and macular pigment densities had little effect on the results presented in this paper. The amount of input from this new S-cone fundamental (added to a 1:1 sum of L- and M-cone fundamentals) required to achieve a B/G of 0.59 was 6.1%, essentially identical to the amount needed from the original S-cone fundamental (6.5%).

**The lens as a difference between monkey and human preretinal filtering.** Macular pigment has been identified as an important contributor to differences between human and monkey spectral sensitivity (Cottaris 2003; Harwerth and Smith 1985; Ingling and Tsou 1977; Sun et al. 2006). However, for cortical neurophysiological recordings, which tend to be made  $>3^\circ$  from the fovea, the lens is the more influential filter. The thickness of the unaccommodated monkey lens is  $\sim 3.4$  mm (Wendt et al. 2008), which is 15% thinner than the equivalent human lens (Rosen et al. 2006). This difference is in the right direction to account for our results: the thinner the lens, the less

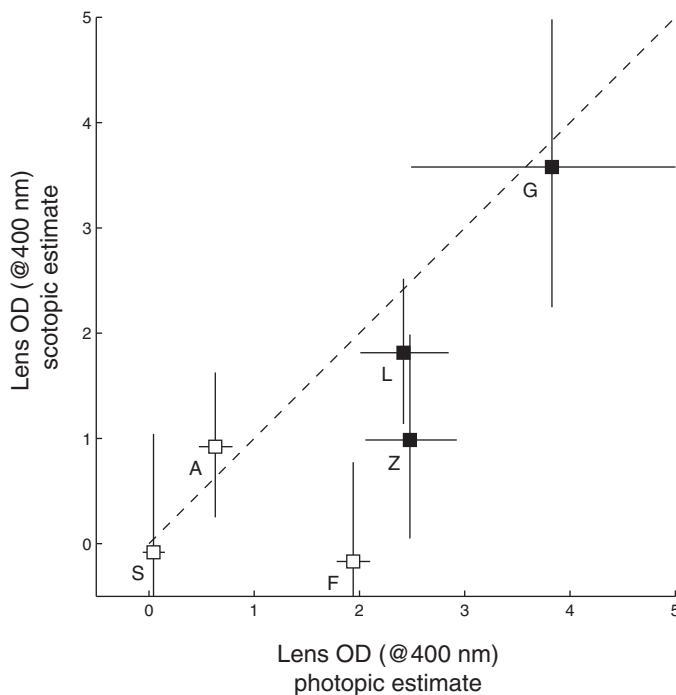


Fig. 6. Lens OD (at 400 nm) estimates derived from photopic and scotopic B/G for three monkey (open symbols) and three human observers (solid symbols). Symbols are means, and error bars are SEs, which were calculated from  $\log_{10}$  B/G and then converted to lens OD. Letters identify individual subjects (see Fig. 3). Dashed line is unity.

light it absorbs. However, a 15% difference is too small to account for the difference in spectral sensitivity we observed between humans and monkeys.

Lenses yellow over time, absorbing more short-wavelength light in older subjects. The monkeys used in vision experiments are typically younger than the humans against whom they are compared. This is consistent with the observation that monkeys in our study were more sensitive to blue than their older, human counterparts. The average age of our monkeys was 6.8 yr, which predicts a lens density of 1.18 at 400 nm, based on juvenile human data (Werner 1982). Multiplying this by 0.85 to account for the 15% difference in the axial length of the monkey and human lenses gives a density of 1.

In this study, we scaled a lens optical density template (Stockman et al. 1999) to adjust a set of human cone fundamentals until they accurately predicted psychophysical data from the monkey. We scaled the lens absorption spectrum rather than manipulating its shape because changes in shape are unconstrained by our data. Nevertheless, the modeling of the monkey lens absorption spectrum as a scaled version of that of the humans is an approximation. The absorption spectrum of the macaque lens may drop more steeply with wavelength than that of the human lens (Boettner 1967; van Norren 1972; van Norren and Vos 1974; Wald 1949; Wyszecki and Stiles 1982), a fact that may be related to lens age (Pokorny et al. 1987; van de Kraats and van Norren 2007). An important future direction is to synthesize a set of cone fundamentals for monkeys that are independent of the human color-matching functions.

*Implications for color experiments in monkeys.* Which set of human-based cone fundamentals are most appropriate for neurophysiological experiments in monkeys? Consistent with Cottaris (2003), we find that the 10° fundamentals are a better choice than the 2° fundamentals. Our study extends this finding to the parafovea, where one might have expected the 2° fundamentals to be superior. The fact that photopic B/G varied only slightly from 2 to 7° within individual monkeys suggests that adjusting the fundamentals as a function of eccentricity is probably unnecessary for most neurophysiology experiments. The greater variance in B/G across monkeys suggests that consideration of inter-monkey differences in preretinal filtering may be important for some neurophysiological studies.

The monkeys' chromatic sensitivity at high temporal frequencies motivates a reconsideration of the relationship between the responses of neurons in the visual cortex and stimulus visibility. Some neurons in the monkey primary visual cortex respond to isoluminant flicker at 15 Hz and above (Gur and Snodderly 1997), and human observers have difficulty detecting these stimuli (Fig. 5 and Swanson et al. 1987). These results have been interpreted as evidence that neurons in the primary visual cortex do not contribute directly to conscious visual perception (Crick and Koch 1998). As we have shown here, monkeys can detect chromatic flicker at higher frequencies than humans can (see also Gagin et al. 2014). The possibility remains that the sensitivity of V1 neurons to rapid chromatic flicker tracks psychophysical sensitivity, as it does at lower temporal frequencies (Hass and Horwitz 2013). Testing this hypothesis rigorously will require simultaneous measurements of neural responses and detection thresholds.

## ACKNOWLEDGMENTS

The authors thank Charlie Hass for computer programming and for providing comments on an early version of the manuscript, and Jessica Rowlan, Jay Neitz, and Maureen Neitz for helpful discussions and electroretinogram measurements. NPRC Bioengineering provided technical support.

## GRANTS

This work was supported by National Institutes of Health Grants EY-018849 (G. D. Horwitz), University of Washington Vision Core Grant P30-EY-01730, and National Center for Research Resources Grant RR-00166.

## DISCLOSURES

No conflicts of interest, financial or otherwise, are declared by the author(s).

## AUTHOR CONTRIBUTIONS

Author contributions: Z.L.-B., L.J.T., and G.D.H. performed experiments; Z.L.-B. and G.D.H. analyzed data; Z.L.-B., L.J.T., and G.D.H. interpreted results of experiments; Z.L.-B. and G.D.H. prepared figures; Z.L.-B. and G.D.H. drafted manuscript; Z.L.-B., L.J.T., and G.D.H. edited and revised manuscript; Z.L.-B., L.J.T., and G.D.H. approved final version of manuscript; G.D.H. conception and design of research.

## REFERENCES

- Baylor DA, Nunn BJ, Schnapf JL. Spectral sensitivity of cones of the monkey *Macaca fascicularis*. *J Physiol* 390: 145–160, 1987.
- Boettner EA. *Spectral Transmission of the Eye*. Brooks Air Force Base, TX: US Air Force School of Aerospace Medicine, 1967.
- Bowmaker JK. Cone visual pigments in monkeys and humans. In: *Advances in Photoreception: Proceedings of a Symposium on Frontiers of Visual Science*. Washington, DC: National Academy, 1990, p. 19–30.
- Bowmaker JK, Dartnall HJ, Lythgoe JN, Mollon JD. The visual pigments of rods and cones in the rhesus monkey, *Macaca mulatta*. *J Physiol* 274: 329–348, 1978.
- Brainard DH. The Psychophysics Toolbox. *Spat Vis* 10: 433–436, 1997.
- Brainard DH, Roorda A, Yamauchi Y, Calderone JB, Metha A, Neitz M, Neitz J, Williams DR, Jacobs GH. Functional consequences of the relative numbers of L and M cones. *J Opt Soc Am A* 17: 607–614, 2000.
- Chang Y, Burns SA, Kreitz MR. Red-green flicker photometry and nonlinearities in the flicker electroretinogram. *J Opt Soc Am A* 10: 1413–1422, 1993.
- Cole GR, Hine T, McIlhagga W. Detection mechanisms in L-, M-, and S-cone contrast space. *J Opt Soc Am A* 10: 38–51, 1993.
- Cottaris NP. Artifacts in spatiochromatic stimuli due to variations in preretinal absorption and axial chromatic aberration: implications for color physiology. *J Opt Soc Am A* 20: 1694–1713, 2003.
- Crawford BH. The scotopic visibility function. *Proc Phys Soc B* 62: 321–334, 1949.
- Crick F, Koch C. Consciousness and neuroscience. *Cereb Cortex* 8: 97–107, 1998.
- Dartnall HJ, Bowmaker JK, Mollon JD. Human visual pigments: microspectrophotometric results from the eyes of seven persons. *Proc R Soc Lond B Biol Sci* 220: 115–130, 1983.
- De Valois RL, Jacobs GH. Primate color vision. *Science* 162: 533–540, 1968.
- De Valois RL, Morgan HC. Psychophysical studies of monkey vision. II. Squirrel monkey wavelength and saturation discrimination. *Vision Res* 14: 69–73, 1974.
- De Valois RL, Morgan HC, Polson MC, Mead WR, Hull EM. Psychophysical studies of monkey vision. I. Macaque luminosity and color vision tests. *Vision Res* 14: 53–67, 1974.
- Eisner A, MacLeod DI. Blue-sensitive cones do not contribute to luminance. *J Opt Soc Am A* 70: 121–123, 1980.
- Eskew RT, McLellan JS, Giulianini F. Chromatic detection and discrimination. In: *Color Vision: From Genes to Perception*. Cambridge, UK: Cambridge University, 1999, p. 345–368.
- Field GD, Gauthier JL, Sher A, Greschner M, Machado TA, Jepson LH, Shlens J, Gunning DE, Mathieson K, Dabrowski W, Paninski L, Litke AM, Chichilnisky EJ. Functional connectivity in the retina at the resolution of photoreceptors. *Nature* 467: 673–677, 2010.



- Gagin G, Bohon KS, Butensky A, Gates MA, Hu JY, Lafer-Sousa R, Pulumo RL, Qu J, Stoughton CM, Swanbeck SN, Conway BR. Color-detection thresholds in rhesus macaque monkeys and humans. *J Vis* 14: 12, 2014.
- Gegenfurtner KR, Hawken MJ. Temporal and chromatic properties of motion mechanisms. *Vision Res* 35: 1547–1563, 1995.
- Gur M, Snodderly DM. A dissociation between brain activity and perception: chromatically opponent cortical neurons signal chromatic flicker that is not perceived. *Vision Res* 37: 377–382, 1997.
- Hall N, Colby C. Psychophysical definition of S-cone stimuli in the macaque. *J Vis* 13: 20, 2013.
- Hammond BR Jr, Wooten BR, Smollon B. Assessment of the validity of in vivo methods of measuring human macular pigment optical density. *Optom Vis Sci* 82: 387–404, 2005.
- Harosi FL. Cynomolgus and rhesus monkey visual pigments. Application of Fourier transform smoothing and statistical techniques to the determination of spectral parameters. *J Gen Physiol* 89: 717–743, 1987.
- Harwerth RS, Smith EL 3rd. Rhesus monkey as a model for normal vision of humans. *Am J Optom Physiol Opt* 62: 633–641, 1985.
- Hass CA, Horwitz GD. Effects of microsaccades on contrast detection and V1 responses in macaques. *J Vis* 11: 1–17, 2011.
- Hass CA, Horwitz GD. V1 mechanisms underlying chromatic contrast detection. *J Neurophysiol* 109: 2483–2494, 2013.
- Horwitz GD, Hass CA. Nonlinear analysis of macaque V1 color tuning reveals cardinal directions for cortical color processing. *Nat Neurosci* 15: 913–919, 2012.
- Inglis CR Jr, Tsou BHP. Orthogonal combination of the three visual channels. *Vision Res* 17: 1075–1082, 1977.
- Jacobs GH, Deegan JF 2nd. Spectral sensitivity of macaque monkeys measured with ERG flicker photometry. *Vis Neurosci* 14: 921–928, 1997.
- Jacobs GH, Deegan JF 2nd. Uniformity of colour vision in Old World monkeys. *Proc Biol Sci* 266: 2023–2028, 1999.
- Kleiner M, Brainard DH, Pelli DG. What's new in Psychtoolbox-3 (Abstract). *Perception* 36, ECVS Suppl: 14, 2007.
- Kodak. *Kodak Photographic Filters Handbook*. Rochester, NY: Eastman Kodak, 1990, p. 132.
- Kremers J, Scholl HP, Knau H, Berendschot TT, Usui T, Sharpe LT. L/M cone ratios in human trichromats assessed by psychophysics, electroretinography, and retinal densitometry. *J Opt Soc Am A* 17: 517–526, 2000.
- Lee BB, Martin PR, Valberg A. Sensitivity of macaque retinal ganglion cells to chromatic and luminance flicker. *J Physiol* 414: 223–243, 1989.
- Pelli DG. The VideoToolbox software for visual psychophysics: transforming numbers into movies. *Spat Vis* 10: 437–442, 1997.
- Poirson AB, Wandell BA, Varner DC, Brainard DH. Surface characterizations of color thresholds. *J Opt Soc Am A* 7: 783–789, 1990.
- Pokorny J, Smith VC, Lutze M. Aging of the human lens. *Appl Opt* 26: 1437–1440, 1987.
- Rosen AM, Denham DB, Fernandez V, Borja D, Ho A, Manns F, Parel JM, Augusteyn RC. In vitro dimensions and curvatures of human lenses. *Vision Res* 46: 1002–1009, 2006.
- Schrier AM, Blough DS. Photopic spectral sensitivity of macaque monkeys. *J Comp Physiol Psychol* 62: 457–458, 1966.
- Sharpe LT, Stockman A, Jagla W, Jagle H. A luminous efficiency function,  $V^*(\lambda)$ , for daylight adaptation. *J Vis* 5: 948–968, 2005.
- Sharpe LT, Stockman A, Jagla W, Jägle H. A luminous efficiency function,  $VD65^*(\lambda)$ , for daylight adaptation: a correction. *Color Res Appl* 36: 42–46, 2011.
- Snodderly DM, Auran JD, Delori FC. The macular pigment. II. Spatial distribution in primate retinas. *Invest Ophthalmol Vis Sci* 25: 674–685, 1984a.
- Snodderly DM, Brown PK, Delori FC, Auran JD. The macular pigment. I. Absorbance spectra, localization, and discrimination from other yellow pigments in primate retinas. *Invest Ophthalmol Vis Sci* 25: 660–673, 1984b.
- Stockman A, MacLeod DI, DePriest DD. The temporal properties of the human short-wave photoreceptors and their associated pathways. *Vision Res* 31: 189–208, 1991.
- Stockman A, Sharpe LT. The spectral sensitivities of the middle- and long-wavelength-sensitive cones derived from measurements in observers of known genotype. *Vision Res* 40: 1711–1737, 2000.
- Stockman A, Sharpe LT, Fach C. The spectral sensitivity of the human short-wavelength sensitive cones derived from thresholds and color matches. *Vision Res* 39: 2901–2927, 1999.
- Sun H, Smithson HE, Zaidi Q, Lee BB. Specificity of cone inputs to macaque retinal ganglion cells. *J Neurophysiol* 95: 837–849, 2006.
- Swanson WH, Ueno T, Smith VC, Pokorny J. Temporal modulation sensitivity and pulse-detection thresholds for chromatic and luminance perturbations. *J Opt Soc Am A* 4: 1992–2005, 1987.
- van de Kraats J, van Norren D. Optical density of the aging human ocular media in the visible and the UV. *J Opt Soc Am A* 24: 1842–1857, 2007.
- van Norren D. Macaque photopic spectral sensitivity. *Vision Res* 11: 1175–1177, 1971.
- van Norren D. Macaque lens absorption in vivo. *Invest Ophthalmol* 11: 177–181, 1972.
- van Norren DV, Vos JJ. Spectral transmission of the human ocular media. *Vision Res* 14: 1237–1244, 1974.
- Wald G. The photochemistry of vision. *Doc Ophthalmol* 3: 94–137, 1949.
- Watson AB, Pelli DG. QUEST: a Bayesian adaptive psychometric method. *Percept Psychophys* 33: 113–120, 1983.
- Wendt M, Croft MA, McDonald J, Kaufman PL, Glasser A. Lens diameter and thickness as a function of age and pharmacologically stimulated accommodation in rhesus monkeys. *Exp Eye Res* 86: 746–752, 2008.
- Werner JS. Development of scotopic sensitivity and the absorption spectrum of the human ocular media. *J Opt Soc Am A* 72: 247–258, 1982.
- Wooten BR, Hammond BR Jr. Spectral absorbance and spatial distribution of macular pigment using heterochromatic flicker photometry. *Optom Vis Sci* 82: 378–386, 2005.
- Wooten BR, Hammond BR, Renzi LM. Using scotopic and photopic flicker to measure lens optical density. *Ophthalmic Physiol Opt* 27: 321–328, 2007.
- Wyszecki G, Stiles WS. *Color Science: Concepts and Methods, Quantitative Data and Formulae*. New York: Wiley, 1982.